A Pinch of Salt Improves n-Butanol Selectivity in the Guerbet Condensation of Ethanol over Cu-doped Mg/Al Oxides

Jacob A. Barrett[§], Zachary R. Jones[†,§], Craig Stickelmaier[†,§], Nora Schopp[‡,§], Peter C. Ford*[,§]

[§]Department of Chemistry & Biochemistry, University of California, Santa Barbara, Santa Barbara, California 93106-9510, USA

[†]Department of Chemical Engineering, University of California, Santa Barbara, Santa Barbara, California 93106-9510, USA

[‡]RWTH Aachen University, Templergraben 55, 52062 Aachen, Germany

ABSTRACT: *The improvement of processes that utilize renewable feedstocks, such as bioethanol, to produce chemicals ordinarily derived from nonrenewable fossil carbon feedstocks is paramount to creating an environmentally sustainable chemical and fuel industry. Catalytic conversion of ethanol via the Guerbet condensation has the potential to serve as a renewable source of chemicals and/or fuel additives from biorefineries. In this contribution, we demonstrate that a single exposure to soluble chloride leads to marked selectivity changes in the products from the ethanol condensation over a copper-doped porous metal oxide catalyst prepared by calcining Cu-doped Mg/Al hydrotalcites. Without this modification, the Guerbet reaction products are ethyl acetate and n-butanol plus some 1-hexanol, butyl acetate, and ethyl butanoate. A single exposure to ppm quantities of a chloride source leads to markedly improved selectivity toward the generation of n-butanol and 1-hexanol and to a moderate activity increase. X-ray diffraction and basicity measurements pre- and post- reaction were used to examine how chloride alters the properties of this Earth-abundant catalyst.*

KEYWORDS: *Guerbet alcohols, ethanol, ethyl acetate, butanol, biofuels, hydrotalcite, porous metal oxide, chloride*

Supporting Information Placeholder

INTRODUCTION

Gasoline constitutes the majority of transportation energy consumed in the United States. The environmental costs of such fossil fuel use led to establishment of the Renewable Fuel Standard (RFS) Program[1] to ensure that transportation fuels contain certain renewable components that would reduce greenhouse gas (GHG) emissions. The RFS program requirements and in part has driven research into the production of lignocellulose-based biofuels, including “second generation” or cellulosic ethanol. Ethanol (EtOH) constitutes the largest portion of biofuels produced in the US and globally.[2]

EtOH is typically mixed with gasoline to produce E10 gasoline (10 % EtOH by volume) which results in increased octane number and combustion efficiency.[3-5] Although most gasoline in the US contains EtOH, the high water solubility and corrosiveness of the latter present challenges in fuel transport and engine structural integrity.[6]

Butanol (n-BuOH) produced from bio-ethanol would be a potential alternative with favorable characteristics including higher energy density (Figure 1) and lower water solubility than EtOH.[6] Furthermore, a recent evaluation of n-butanol, isobutanol, ethanol, methanol, and acetone-gasoline fuel blends in spark-ignition engines showed that the butanol blends provided the greatest GHG emission reduction amongst the blends evaluated.[7]

The Guerbet condensation of EtOH is an established pathway to the production of n-BuOH and higher alcohols[8] that are also industrially useful chemicals.[9,10] The Guerbet condensation reaction has been known for over a century.[11] However, as noted in a recent review by Galadima and Muraza,[12] selectivity improvements are necessary to enhance this reaction’s applicability to a sustainable chemical and/or fuel industry,

Among catalysts for the Guerbet reaction are transition metal doped porous metal oxides (PMOs) derived by calcining doped Mg^{2+}/Al^{3+} hydrotalcites.[14-20] Ethyl acetate (EtOAc) is a major byproduct of the ethanol condensation catalyzed by such PMOs,[19] but, while it is a useful solvent, EtOAc has a lower specific energy content as a fuel than does EtOH or n-BuOH.[21] The present manuscript describes a chloride-modified Cu-doped PMO catalyst for the Guerbet reaction that provides greater selectivity toward n-BuOH production.

This laboratory[22-25] and, subsequently, others[26] have shown that copper-doped PMOs derived from the calcination of Cu-doped 3/1 Mg^{2+}/Al^{3+} hydrotalcites are effective catalysts for the reductive disassembly of lignin and of lignocellulose in super-critical methanol (sc-MeOH) or ethanol (sc-EtOH). Recently, similar CuPMOs have seen application in the Guerbet reaction; for example, Sun et al achieved good ethanol conversions and n-butanol yields using Cu/Ni doped PMOs.[27] In an ongoing study,[28,29] we have found that small amounts of chloride impurities in lignin substrates (or added separately) led to changes in catalyst activity and attributed those effects to chloride-induced sintering and poisoning of surface metallic Cu sites. The present project was initiated with the goal of evaluating the impact of added chloride salts on the CuPMO catalyzed Guerbet reaction of EtOH. There is indeed an effect, but, remarkably, adding small quantities of chloride salts increases the activity and, more importantly, improves the selectivity of the product stream toward n-BuOH and butanol derived products.[30] Additionally, various butanol derived products also have higher energy density than ethanol (Figure 1) and have potential as renewable fuel additives.

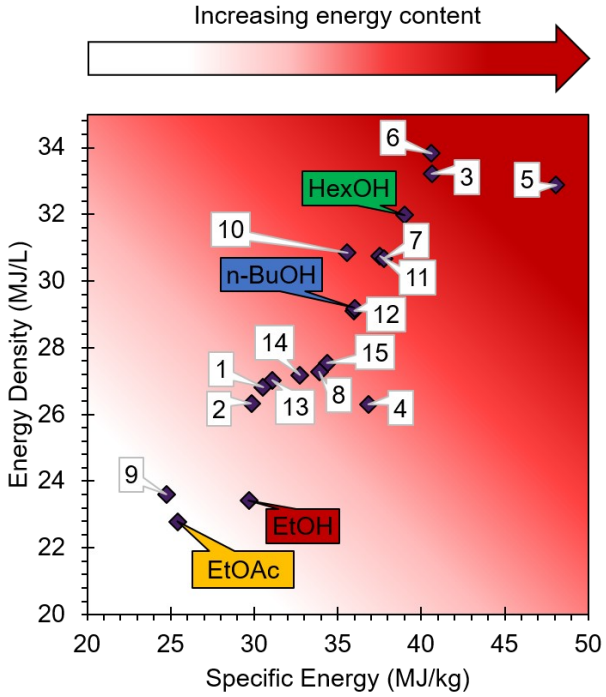

Figure 1. Energy density (MJ/L) and specific energy (MJ/kg) of ethanol and ethanol condensation products calculated using NIST condensed phase thermochemical data.[13] EtOAc = ethyl acetate, EtOH = ethanol, n-BuOH = n-butanol, HexOH = 1-hexanol. Numbered entries are minor products: 1 = ethyl butanoate, 2 = butyl acetate, 3 = 1-octanol, 4 = diethyl ether, 5 = heptane, 6 = 2-ethyl-1-hexanol, 7 = 2-pentanol, 8 = 2-butanone, 9 = butanoic acid, 10 = ethyl octanoate, 11 = 3-hexanone, 12 = 2-pentanone, 13 = butyl butanoate, 14 = 1,1-diethoxyethane, 15 = butyraldehyde.

The Guerbet reaction involves dehydrogenation of an alcohol to an aldehyde, followed by an aldol condensation to an α,β-unsaturated aldehyde. Hydrogenation gives the longer chain alcohol. With ethanol as the substrate, acetaldehyde and crotonaldehyde are key intermediates (Scheme 1).[8,31,32] Acetaldehyde also reacts with ethanol to give the hemiacetal 1-

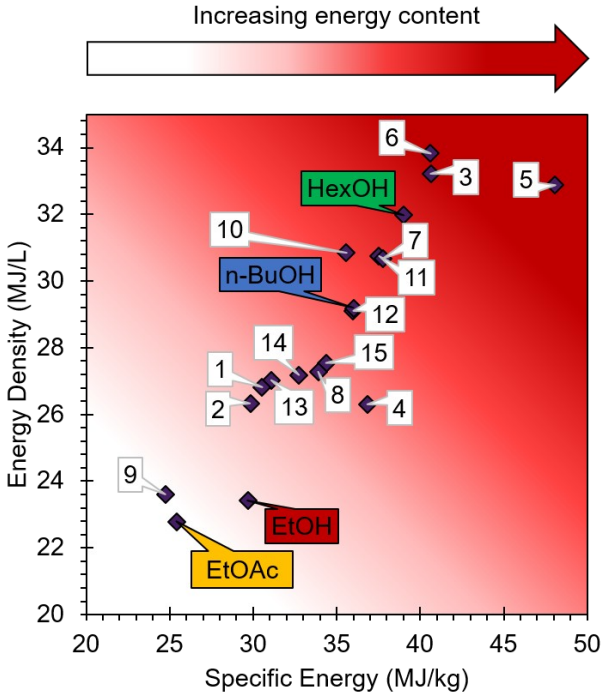

Figure 2. Energy density (MJ/L) and specific energy (MJ/kg) of ethanol and ethanol condensation products calculated using NIST condensed phase thermochemical data.[13] EtOAc = ethyl acetate, EtOH = ethanol, n-BuOH = n-butanol, HexOH = 1-hexanol. Numbered entries are minor products: 1 = ethyl butanoate, 2 = butyl acetate, 3 = 1-octanol, 4 = diethyl ether, 5 = heptane, 6 = 2-ethyl-1-hexanol, 7 = 2-pentanol, 8 = 2-butanone, 9 = butanoic acid, 10 = ethyl octanoate, 11 = 3-hexanone, 12 = 2-pentanone, 13 = butyl butanoate, 14 = 1,1-diethoxyethane, 15 = butyraldehyde.

ethoxyethan-1-ol, dehydrogenation of which forms ethyl acetate (Scheme 2). Other likely side products are diethyl ether, butyl acetate formed by transesterification and longer chain alcohols and esters. All these products have commercial applications as fuels, solvents, plasticizers, etc.[21,33,34] The ability to tailor the product selectivity of this process would provide additional pathways toward ethanol valorization.[14,18,34]

Scheme 1. Plausible pathway for the catalytic conversion of EtOH to n-BuOH with transition metal doped PMOs.[8,31,32]

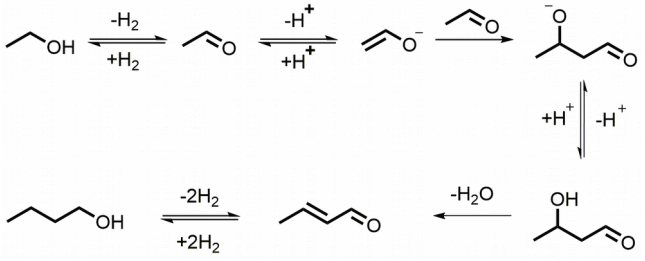

Scheme 2. Plausible pathway for the conversion of EtOH to EtOAc showing the plausible intermediates.

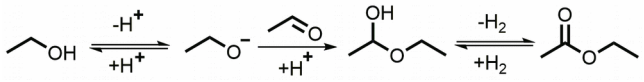

RESULTS AND DISCUSSION

Reactivity and selectivity: Studies were conducted in closed 10 mL mini-reactors constructed from Swagelok junctions[22] to which were added the substrate (typically 2.5 mL 100 % ethanol), the catalyst (typically 100 mg), and an internal standard (20 µL decane). The sealed reactors were placed in a preheated calibrated oven (in most cases at 320 °C), for a specific time period, after which these were removed from the oven and rapidly cooled. The reactor was then opened (caution, these are generally under pressure), and the solution was removed for analysis. The solution components were identified by gas chromatography with mass spectrometric detection (GC-MS) and analyzed quantitatively by gas chromatography with flame ionization detection (GC-FID) as described in the Experimental section of the Supporting Information (SI). Temporal catalysis experiments involved preparing a set of identically loaded mini-reactors that were placed together in the calibrated oven and individually removed at specific time periods. The catalyst in each case was the Cu-doped porous metal oxide (Cu_{20}PMO) prepared by 600 °C calcination of a 3:1 Mg^{2+}/Al^{3+} hydrotalcite (HTC) having 20% of the Mg^{2+} replaced by Cu^{2+}.

Figure 2 compares the results of two such catalysis experiments, one being the reaction of pure EtOH (2.5 mL 200 proof) at 320 °C for 6 h with Cu_{20}PMO (100 mg), the other being the same conditions except a small amount of magnesium chloride was added (0.3 mg $MgCl_2 \bullet 6H_2O$ per 1 mL of EtOH). In the absence of this additive, substrate conversion was 43% but this increased to 59% with the added $MgCl_2 \bullet 6H_2O$ (SI Tables S1 and S2). More importantly, the product distributions changed (yields calculated as described below taking into account the reaction stoichiometry). In the former case, the principal products were EtOAc (16%) and n-BuOH (10%), while identified secondary products were ethyl butanoate (3%) and butyl acetate (2%), consistent with related studies by Sun et al.[27] The selectivity for conversion of EtOH to EtOAc was 45% while that for n-butanol was 29%. The mass balance for this experiment was 93%.

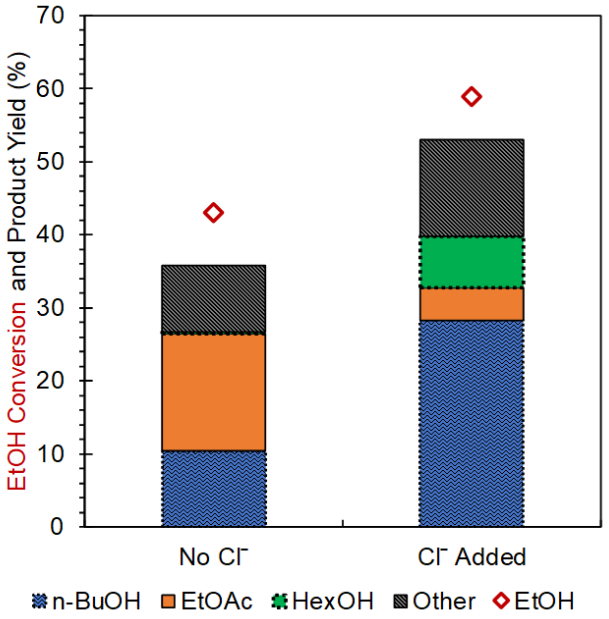

Figure 2. Product yield (%) and ethanol conversion (%, red rhombi) after reaction of ethanol with Cu_{20}PMO for 6 h at 320 °C. Catalyst loading was 5 wt. % (100 mg). 'Cl⁻ Added' corresponds to ethanol with $MgCl_2 \bullet 6H_2O$ added (~140 ppm Cl^-). "Other" products included 1-hexanol, 2-ethyl-1-butanol, ethyl butanoate, butyl acetate, and other C_4+ compounds (see SI Tables S1 & S2).

For the latter reaction, carried out with the addition of a small quantity of $MgCl_2 \bullet 6H_2O$, the increased conversion was accompanied by a remarkable change in selectivity. The yield of n-butanol increased to 28% (53% selectivity) while that of ethyl acetate decreased to 5% (8% selectivity). After n-BuOH the most prominent product was 1-hexanol (13% selectivity), while ethyl butanoate and butyl acetate were observed in yields of ~2% each (SI Tables S1 & S2). The production of n-butanol corresponds to a space time yield of 748 $g_{n\text{-}BuOH}\ kg_{cat}^{-1}\ h^{-1}$, which is slightly higher than that observed by Sun et al using Cu and Ni doped PMOs.[27] The mass balance for this experiment was 94%.

Notably, similar increases in catalyst activity and n-BuOH selectivity were also observed when CCl_4 was instead added as a chloride source.[35] An analogous reaction of EtOH to which $Mg(NO_3)_2$ had been added (50 ppm Mg^{2+}) gave a product distribution nearly identical to that seen in the absence of any additive (SI Figure S1). Thus, we can conclude that it is chloride, not magnesium, that is effecting the increased activity and changes in selectivity toward ethanol oligomerization.

When 95% EtOH (190 proof) was the substrate, conversion under the standard conditions (100 mg Cu_{20}PMO, 6 h reaction at 320 °C) dropped to ~32% with EtOAc remaining the principal product (SI Figure S2). Although adding Cl^- (140 ppm in the form of $MgCl_2 \bullet 6H_2O$) increased conversion to ~39%, the n-BuOH yield (10%) unfortunately remained low. Attempts to modify the conditions by adding dried 3Å molecular sieves (20 wt%) to the batch reactor

did not improve EtOH conversion or BuOH selectivity (SI Figure S2).

Figure 3 illustrates the effects of varying the Cl^- concentration in the substrate solution over the range from 0 to 630 ppm Cl^-. The catalyst was Cu_{20}PMO (100 mg), and the reaction time was 6 h at 320 °C. At the lower chloride concentrations (72-297 ppm), ethanol conversion was ~60% with the selectivity toward n-butanol (~55%) and hexanol (~15%) highest for the runs at 140 and 297 ppm Cl^-. At higher chloride concentrations, the conversion decreased although the net selectivity toward n-BuOH remained similar (~51%).

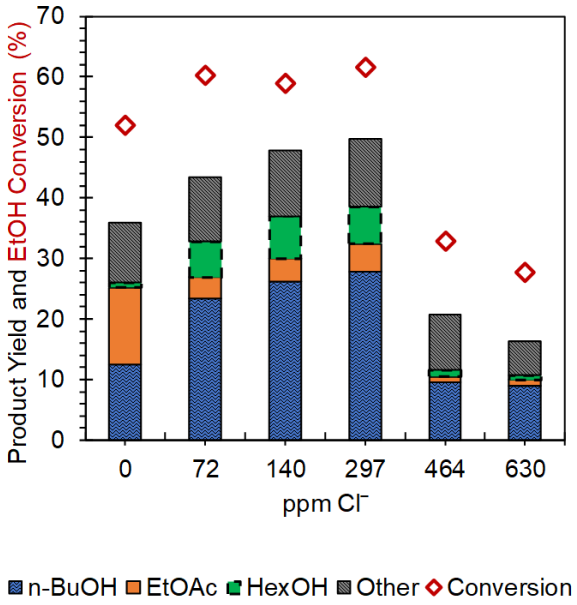

Figure 3. Product yield (%), ethanol conversion (%), and product distribution as a function of added chloride (ppm Cl^-) in the reaction with Cu_{20}PMO for 6 hours at 320 °C. $MgCl_2 \cdot 6H_2O$ was the chloride source. The yields of butanol, ethyl acetate, and hexanol are depicted as blue, orange, and green, respectively. Other, depicted as gray, corresponds primarily to butyl acetate and ethyl butanoate. Red diamonds represent EtOH conversion. These data are the averages of two independent experiments (SI Table S3).

The stability of the catalyst modified by a single exposure to chloride was evaluated in the following manner. The first catalytic run was conducted with Cu_{20}PMO for 6 h at 320 °C with 100% EtOH containing 140 ppm chloride as the substrate. The subsequent 17 runs used the same catalyst recovered in each case by removing the reaction solution for analysis, drying the catalyst in the reactor in vacuo, and reintroducing fresh EtOH as substrate without any added salt. Substrate conversion, ethanol conversion, and n-BuOH selectivity remained high and relatively consistent (Figure 4 and SI Table S4), although with some unexplained variations. Thus, catalyst modification by chloride during the initial run appeared permanent and was not washed away in subsequent reactions with ethanol.

In contrast, when a sequence of seven batch reactor runs was carried out with fresh 100% EtOH containing 140 ppm Cl^- in each run, the activity of the CuPMO catalyst decreased over the first four successive runs until it was about 1/3 of that seen for the first one (SI Figure S3 & Table S5). Notably, the selectivity for n-BuOH over EtOAc remained high. The activity and selectivity for sequential runs with chloride-free EtOH and recovered Cu_{20}PMO remained consistent with that seen in Figure 2 (40-50% EtOH conversion, product yields: ~15% ethyl acetate and ~10% butanol; SI Figure S4 & Table S6).

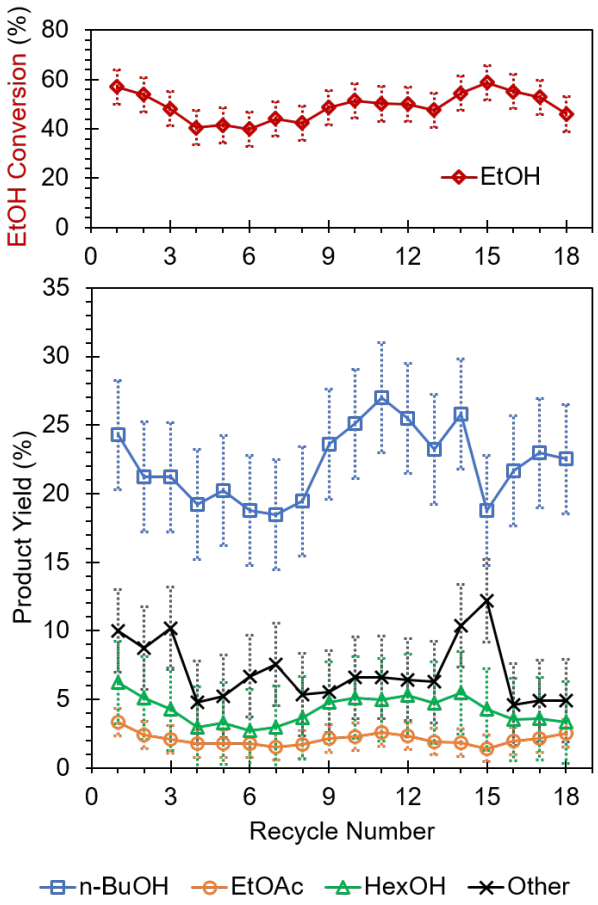

Figure 4. Product yield and ethanol conversion (%) as a function of reaction recycle number. For the first run, the substrate was 100% EtOH (2.5 mL) containing 140 ppm Cl^-. For the subsequent recycles 100% EtOH containing no added chloride was used. Markers represent the mean value of duplicate experiments run in parallel and the Y-axis error bars represent one standard deviation from the mean. Other products included butyl acetate, ethyl butanoate, 1-octanol. (see SI for all observed products)

Among other parameters explored, higher catalyst loading gave, as expected, higher net conversion for a fixed 6 h reaction time (Figure 5). However, there were only modest effects on the selectivity. The highest n-BuOH selectivity (59%) was seen with 50 mg of Cu_{20}PMO, but nearly the same selectivity (55 %) was seen with catalyst loadings of 75 and 100 mg.

The distribution of products as a function of reaction time is shown in SI Figures S5 and S6. The highest selectivity toward n-BuOH occurred at low conversion. SI Figure S5 (Table S7) shows a time

course with 50 mg Cu_{20}PMO at 320 °C while SI Figure S6 (Table S8) shows a time course with 100 mg Cu_{20}PMO at 300 °C. A 29 % yield of butanol was obtained after 6 h at 320 °C and 26% at 300 °C. The selectivity toward n-BuOH was only slightly higher at 300 °C. The 8 h run at 300 °C had 2% greater EtOH conversion than the 6 h run but did not lead to a higher net n-BuOH yield owing to secondary reactions of n-BuOH to form C_6+ products (Table S8), the majority of which are 1-hexanol, ethyl butanoate, butyl acetate, and 2-ethyl-1-butanol.

The initial ethanol volume in the batch reactor had only a modest effect on the product distribution and was evaluated in a set of batch reactions with 1.5, 2.0, 2.5 mL EtOH with added Cl^- (140 ppm added as $MgCl_2 \cdot 6H_2O$, SI Figure S7). Interestingly, conversion also remained essentially constant at ~55-60%, regardless of the initial quantity of ethanol.

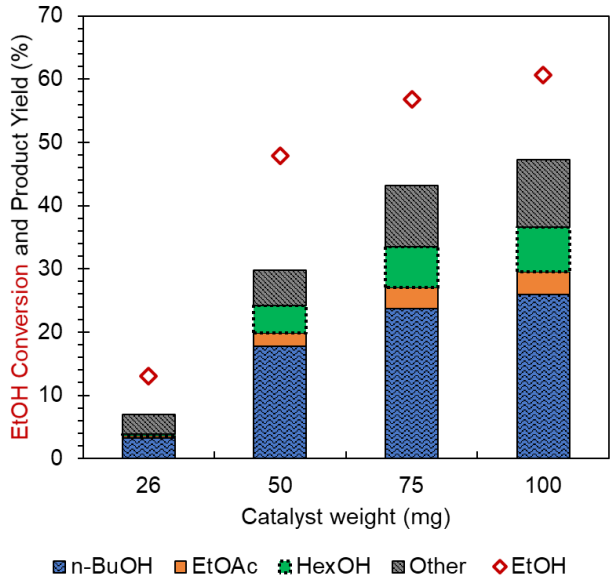

Figure 5. Product yield and ethanol conversion (%) as a function of catalyst loading. Reaction of 2.5 mL of ethanol (140 ppm Cl^-) with Cu_{20}PMO for 6 h at 320 °C. Other products are mainly butyl acetate and ethyl butanoate.

Catalyst characterization: In order to gain insight into chloride-induced structural changes, we examined the X-ray diffraction (XRD) patterns of the post-reaction catalysts from the experiment shown in Figure 3 (Figure 6). Reference patterns can be found in SI Figures S8 & S9. As seen previously,[22] calcination transforms Cu-doped HTC to an amorphous PMO. The XRD pattern for freshly calcined Cu_{20}PMO (trace A, Figure 6) shows only broad Bragg reflections at 36°, 43°, and 63° 2Θ consistent with some MgO domains. After reaction with ethanol for 6 h at 320 °C (trace B), new reflections at 11°, 22°, 35°, 39°, 60°, and 61° are seen that suggest partial restoration of a hydrotalcite structure, possibly due to H_2O formation as a byproduct of the ethanol condensation (Scheme 1). An alternative assignment for the reflections at 35° and 39° would be to CuO domains, while reflections at 36°, 42°, 51°, 62° and 73° correspond to Cu_2O; however, these overlap with the broad reflections for MgO domains noted above.

After the catalytic run carried out with 72 ppm Cl^- in EtOH, presence of a $Mg(OH)_2$ is suggested by the reflections at 19° and 38°, although there is much overlap between a Mg/Al layered double hydroxide and $Mg(OH)_2$. It is likely that gibbsite, $Al(OH)_3$ and/or Al(O)OH, is also formed in the presence of brucite, $Mg(OH)_2$. However, not all the Bragg reflections for Al-containing phases were observed. The reflections at 35° and 39° are assigned to CuO as other reflections at 51°, 59°, and 69° characteristic of this solid are also seen. The large reflection at 44°, overlapping reflection at 51°, and reflection at 74° correspond to metallic copper (Cu^0). The formation of copper nanoparticles has been previously observed for Cu_{20}PMO in the reaction of bio-oil sugar fractions in supercritical alcohols using transmission electron microscopy (TEM).[36] Additionally, Sun et al observed spherical metal nanoparticles by TEM for Cu/Ni doped PMO after the Guerbet reaction of ethanol.[27]

The XRD pattern for the recovered catalyst after runs with ethanol containing 140 ppm Cl^- (trace D) or 297 ppm Cl^- (trace E) were nearly identical. However, the recovered catalyst after runs at higher chloride concentrations (464 or 630 ppm Cl) displayed much larger reflections at 44°, 51°, and 74° corresponding to more Cu metal domains (traces F & G) as compared to lower chloride concentrations. The broad reflections for MgO are also still observed as well as ones at 11° and 22°. Clearly, increased chloride concentration resulted in increased Cu sintering.

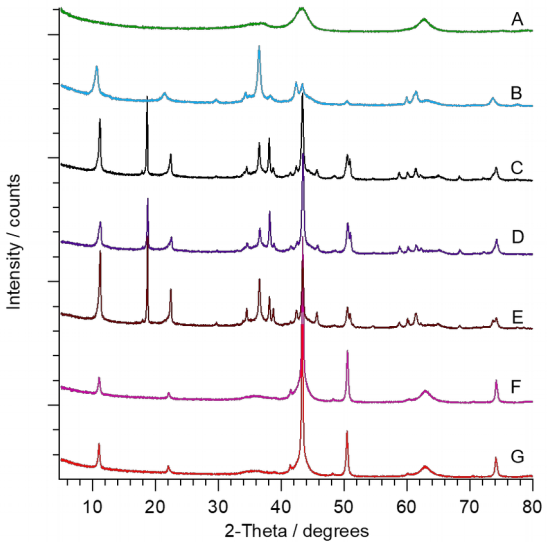

Figure 6. XRD of Cu_{20}PMO catalysts after calcination at 600° (A, green) and after reaction with EtOH at 320 °C for 6 h (in descending order) under the following conditions: (B) no chloride, (C) 72 ppm Cl^-, (D) 140 ppm Cl^-, (E) 297 ppm Cl^-, (F) 464 ppm Cl^- and (G) 630 ppm Cl^-. All data analysis was done using Malvern Panalytical HighScore Software with two structural databases; Inorganic Crystal Structure Database and Powder Diffraction Files.

The Cu crystallite domain sizes can be roughly estimated from the Bragg reflection width at 44° 2Θ using the Scherer equation.[37] Typically all reflections corresponding to a crystallite should be used for such estimates, however, overlaps of some

reflections made this impractical. Accordingly, the Cu domain size was estimated from the traces shown in Figure 6 to be 25 nm for the catalyst after runs at 140 and 297 ppm Cl^- and 24 nm after the run at 72 ppm Cl^-. A larger Cu crystallite size (29 nm) was found after runs at higher chloride concentration (464 or 630 ppm). In contrast the XRD pattern for the Cu_{20}PMO recovered after reaction with EtOH containing no chloride gave only a very small reflection at 44° too weak to extract a meaningful crystallite size approximation. All catalyst samples with chloride exhibited Bragg reflections consistent with Cu metal, however, the catalyst examined after reaction with ethanol containing 42-297 ppm Cl^- also exhibits reflections consistent with CuO and Cu_2O. Given that these catalysts were more active than those with higher chloride concentration (464 or 630 ppm), one might speculate that Cu oxide domains are involved in the observed increased activity. ~~Given that reactions with chloride as an additive in the range of 72-297 ppm produce a more active catalyst with excellent selectivity for n-butanol formation, one might speculate that the active site involves copper nanoparticles with multiple valencies (Cu/CuO/Cu_2O) on a $Mg(OH)_2$/ mixed with a composite $Mg(Al)O_x$.~~

Notably, the XRD pattern (SI Figure S10) of the recovered catalyst after a single run with added chloride followed by 17 successive runs with ethanol alone, as detailed above, appears remarkably similar to that observed in Figure 6 after only a single run with the same amount of Cl^-. However, according to the full-width half maximum (FWHM) at 44° 2Θ, the estimated Cu domain size increased to 27 nm. The catalyst sample from the reaction with EtOH without chloride exhibited the same surface area but decreased pore volume and size (Table 1). However, the BET surface area of reacted catalysts generally decreased after reaction. These results are consistent with the formation of large Cu domains. Cu_{20}PMO that was reacted with EtOH containing chloride exhibited a lower surface area than catalyst that reacted with pure EtOH. This is in agreement with the formation of layered phases implied by the XRD patterns.

Table 1. N_2 adsorption analysis of Cu_{20}PMO catalysts after calcination and/or reaction with EtOH at 320 °C for 6 h.

Sample Conditions	BET surface area (m^2/g)	pore volume (cm^3/g)	pore size (nm)
Calcined 600°C	135	0.70	10.5
No chloride	137	0.45	6.1
72 ppm Cl^-	101	0.41	7.4
140 ppm Cl^-	97	0.47	8.2
267 ppm Cl^-	67	0.36	9.6
464 ppm Cl^-	69	0.55	13.9
630 ppm Cl^-	84	0.62	12.7
7 runs (no chloride)	77	0.43	9.9

In an earlier study with bioethanol, Marcu et. al showed that the addition of water to CuPMOs decreases catalytic activity.[16] The rationale for this observation was that Lewis base O^{2-} sites are transformed into ^-OH sites in the presence of water. Water may also play a role in Cu metal sintering. After the run with 95% EtOH containing 140 ppm Cl^-, the Cu domain size calculated from the XRD was 33 nm (SI Figure S11). For comparison, the XRD patterns reacted consecutively with pure ethanol show that layered double hydroxide structure indicated by 11°, 22°, 60°, 61° largely disappears after 7 consecutive 6 h reactions (SI Figure S12). This is also true for the catalyst of the 18th 6 h reaction shown in SI Figure S10. In both cases the reflections at 19° and 38°, assigned as $Mg(OH)_2$ is present. Formation of H_2O as indicated in Scheme 1 may contribute to rehydration of the PMO to a hydrotalcite.[38,39]

The ATR-infrared spectrum was recorded for each Cu_{20}PMO sample for which XRD patterns are shown in Figure 6. In the 4,000-1,000 cm^{-1} range, the spectrum of freshly calcined catalyst displays only broad, weak bands at ~3,400 cm^{-1} and ~1500 cm^{-1} that may represent surface water and carbonate, respectively (SI Figure S13). The IR spectra recorded after 6 h reactions with ethanol at 320 °C containing different chloride concentrations show distinct changes. In each case, the IR spectrum shows an enhanced broad band at ~3600 cm^{-1} corresponding to surface water and weaker but sharper bands at 2950, 2900 and 2850 cm^{-1} consistent with C-H stretches, indicating that organic molecules remain on the catalyst surface even after subjection to a vacuum for several days. Two stronger bands at ~1575 and ~1411 cm^{-1} are also apparent. These do not represent interstitial water since the H-O-H bending vibrations typically are seen at ~1640 cm^{-1} for hydrotalcites and ~1630 cm^{-1} for brucite.[40,41] Carbonate shows bands at 1365/1400 cm^{-1} in hydrotalcites,[42] at 1515 cm^{-1} for brucite,[43] and at 1520 and 1430 cm^{-1} for aluminum hydroxy carbonate.[44] A better fit is acetate, which displays bands at 1554 and 1428 cm^{-1} on a ZnO surface.[45]

PMO basicity is a characteristic that has been correlated with ethanol condensation selectivity and activity.[14] The Hammett acidity function (H_) in conjunction with pH indicators to determine the solid basicity of select catalysts (Table 2). The Cu_{20}PMO catalyst reacted with EtOH which contained 140 ppm Cl^- has greater total basicity (1.90 mmol/g) than catalyst reacted with EtOH containing no chloride (1.34 mmol/g). Though, the overall base strength for Cu_{20}PMO reaction with EtOH containing 140 ppm Cl^- is lower, as this catalyst was unable to ionize nile blue (pKa = 10.1).

Table 2. Hammett basicity (H_) of Cu_{20}PMO catalysts after calcination and/or reaction with EtOH at 320 °C for 6 h.

Sample Conditions	Base strength	Total basicity (mmol/g)
Calcined 600°C	10.1<H_<15	1.07 ± 0.10

No chloride	10.1<H_<15	1.34 ± 0.26
140 ppm Cl^-	9.3<H_<10.1	1.90 ± 0.20

A key first step toward both products would be ethanol dehydrogenation to acetaldehyde. The formation of n-butanol depends on deprotonation of acetaldehyde to form an enolate which then condenses with another acetaldehyde molecule to form a C-C bond and a C_4 chain (Scheme 1). EtOAc formation depends on the reaction of acetaldehyde with ethoxide to form the hemiacetal precursor that undergoes dehydrogenation (Scheme 2). Since, acetaldehyde is several orders of magnitude more acidic than ethanol,[46] we hypothesize that the chloride modification of the Cu_{20}PMO reduces the base strength of the catalyst but increases the total basicity. This **suggestion** is consistent with an increase in EtOH conversion but overall decrease in EtOAc formation since theoretically less ethoxide would form on a catalyst with lower base strength. Perhaps the reduction and sintering of copper oxide into Cu metal nanoparticles and formation of hydroxide phases contribute to the decrease in base strength.

SUMMARY:

We have shown that the addition of relatively small quantities of chloride modifies the activity and selectivity of the products generated via the Guerbet reaction of ethanol with Cu-doped PMOs at 320 °C. Thus, although halogens are known poisons for Cu catalysts,[47,48] added Cl^- in this case increases overall reactivity toward ethanol condensation to n-butanol and its derivatives and suppresses formation of ethyl acetate, which is the predominant product under these conditions in the absence of such catalyst modification.

The enhancement in selectivity and conversion for ethanol condensation as catalyzed by mixed metal oxide catalysts realized in this study is progress towards renewable feedstock derived n-butanol. BuOH can potentially serve as an important chemical precursor or advanced biofuel in a biobased economy. In addition, our results show that specific adsorbates like chloride can be useful in tuning selectivity for the development of mixed phase catalysts for the Guerbet condensation reaction.

MATERIALS AND METHODS:

The PMO catalyst was prepared by calcination of the copper-doped hydrotalcite prepared by coprecipitation.[17-19] In short, a solution of Cu^{2+}, Mg^{2+}, and Al^{3+} nitrates with the cationic stoichiometric ratio 0.6/2.4/1.0 were slowly added to aqueous Na_2CO_3 at 60 °C while keeping pH between 8 and 10 using aqueous NaOH. The resulting light blue slurry was stirred for 3 days at 60 °C, cooled, and filtered. The resulting solid was resuspended in aqueous Na_2CO_3 for 1 day at room temperature, then washed copiously with deionized water, and dried in vacuo. Catalyst composition was verified by ICP-AES using a ThermoiCAP 6300 ICP equipped with a 6000 K Ar plasma and confirmed that 20% of the dications in the resulting 3/1 hydrotalcite were Cu^{2+}. These materials have been designated as Cu_{20}HTCs. Calcination of the Cu_{20}HTC for 18 h at 600 °C gave the Cu_{20}PMOs used as catalysts.

PMO catalysts were characterized by powder XRD, BET surface area analysis, and ATR-IR. Powder XRD was performed on a Panalytical Empyrean Diffractometer, with Cu Kα radiation (λ= 1.5405980 Å) in a zero-background sample holder. Infrared spectra were collected on a Bruker ALPHA FTIR instrument with diamond ATR module. Surface area, pore volume, and pore size was measures using a MicroMeritics TriStar Porosimeter. Approximately 100 mg of catalyst sample was degassed under N_2 overnight at 200 °C after which the adsorption isotherm data was collected. Attenuated total reflectance infrared (ATR-IR) spectra were collected on a Bruker ALPHA FT- IR instrument equipped with a diamond ATR module.

Compounds were identified using GC-MS, Hewlett Packard 5890, and quantified via GC-FID, Agilent 6890N (G1530N), using the Effective Carbon Number (ECN) methodology.[49,50] Yield for each product was calculated according to eq. 1,

$$Yield\,(\%) = \frac{SF\,x\,mol_{product}}{mol\,EtOH_{initial}} \times 100 \quad (1)$$

where SF is the stoichiometric factor (e.g. 2 moles of EtOH are required to form 1 mole of n-butanol), $mol_{product}$ is the amount of product detected, and $mol\ EtOH_{initial}$ is amount of EtOH initially added to the reactor.

Percent conversion was calculated according to eq. 2.

$$Conversion\,(\%) = \frac{mol\,EtOH_{converted}}{mol\,EtOH_{initial}} \times 100 \quad (2)$$

where $mol\ EtOH_{converted}$ equals $mol\ EtOH_{initial}$ – $mol\ EtOH_{unreacted}$ and $mol\ EtOH_{unreacted}$ is the EtOH found to remain after the reaction. Mass balance (MB) was calculated according to eq. 3.

$$MB\,(\%) = \frac{\sum (SF\,x\,mol_{products}) + ¿\,mol\,EtOH_{unreacted}}{mol\,EtOH_{initial}} \times 100 \quad (3)$$

Basicity of catalysts was evaluated using Hammett indicators, which has been previously applied for measuring solid basicity.[51] The Hammett indicators used were neutral red (pKa = 6.8), bromothymol blue (pKa = 7.2), phenolphthalein (pKa = 9.3), nile blue (pKa = 10.1), and 2,4-dinitroaniline (pKa = 15). The Hammett acidity function (H_-) describes the ability of the solid to ionize the aforementioned weak acid indicators. The H_- of the solid is considered to be between the pKa of the indicator it can ionize and the indicator it cannot

ionize. The total basicity (mmol/g) was calculated by titration of a 25 mg sample, dissolved in 2 mL of methanol with neutral red indicator, by a 0.01 M Benzoic acid solution in methanol.

ASSOCIATED CONTENT

Supporting Information

The Supporting Information is available free of charge on the ACS Publications website.

AUTHOR INFORMATION

Corresponding Author

*P. C. Ford; Email: ford@chem.ucsb.edu

ORCID

Jacob Barrett: 0000-0002-7522-5699
Peter C. Ford: 0000-0002-5509-9912

Author Contributions

Notes

The authors declare no competing financial interests.

ACKNOWLEDGMENT

J.A.B. acknowledges the US National Science Foundation Graduate Research Fellowship Program for funding. We also thank Lisa Stamper for ATR-IR usage and Susannah Scott for permitting use of GC-MS. The authors also acknowledge the MRL Shared Experimental Facilities which are supported by the MRSEC Program of the NSF under Award No. DMR 1720256; a member of the NSF-funded Materials Research Facilities Network.

REFERENCES

(1) U.S. Environmetal Protection Agency, Renewable Fuel Standard Program: Standards for 2018 and Biomass-Based Diesel Volume for 2019, *Fed Regist.* **2017**, 82 (237), 58486-58527
(2) BP. *BP Statistical Review of World Energy 2017*; 2017.
(3) Agarwal, A. K. Biofuels (Alcohols and Biodiesel) Applications as Fuels for Internal Combustion Engines. *Prog. Energy Combust. Sci.* **2007**, *33* (3), 233–271.
(4) U.S. Environmetal Protection Agency, Partial Grant of Clean Air Act Waiver Application Submitted by Growth Energy To Increase the Allowable Ethanol Content of Gasoline to 15 Percent, *Fed Regist.* **2011**, 76 (17), 4662–4683.
(5) Alleman, T. L.; McCormick, R. L.; Yanowitz, J. Properties of Ethanol Fuel Blends Made with Natural Gasoline. *Energy and Fuels* **2015**, *29* (8), 5095–5102.
(6) Jin, C.; Yao, M.; Liu, H.; Lee, C. F. F.; Ji, J. Progress in the Production and Application of N-Butanol as a Biofuel. *Renew. Sustain. Energy Rev.* **2011**, *15* (8), 4080–4106.
(7) Elfasakhany, A. Investigations on Performance and Pollutant Emissions of Spark-Ignition Engines Fueled with N-Butanol–, Isobutanol–, Ethanol–, Methanol–, and Acetone–gasoline Blends: A Comparative Study. *Renew. Sustain. Energy Rev.* **2017**, *71*, 404–413.
(8) Gabriëls, D.; Hernández, W. Y.; Sels, B.; Van Der Voort, P.; Verberckmoes, A. Review of Catalytic Systems and Thermodynamics for the Guerbet Condensation Reaction and Challenges for Biomass Valorization. *Catal. Sci. Technol.* **2015**, *5*, 3876–3902.
(9) Angelici, C.; Weckhuysen, B. M.; Bruijnincx, P. C. A. Chemocatalytic Conversion of Ethanol into Butadiene and Other Bulk Chemicals. *ChemSusChem* **2013**, *6* (9), 1595–1614.
(10) Falbe, J.; Bahrman, H.; Lipps, W.; Mayer, D.; Frey, G. D. Aliphatic Alcohols. In *Ullmann's Encyclopedia of Industrial Chemistry*; 2013.
(11) Guerbet, M. Action of alcohols on their sodium derivatives. *C. R. Acad. Sci. Paris* **1899**, 128, 1002−1004
(12) Galadima, A.; Muraza, O. Catalytic Upgrading of Bioethanol to Fuel Grade Biobutanol: A Review. *Ind. Eng. Chem. Res.* **2015**, *54* (29), 7181–7194.
(13) *NIST Chemistry WebBook, NIST Standard Reference Database Number 69*; Linstrom, P. J., Mallard, W. G., Eds.; National Institute of Standards and Technology, Gaithersburg MD, 20899, 2017
(14) Di Cosimo, J. I.; Díez, V. K.; Xu, M.; Iglesia, E.; Apesteguía, C. R. Structure and Surface and Catalytic Properties of Mg-Al Basic Oxides. *J. Catal.* **1998**, *178* (2), 499–510.
(15) Di Cosimo, J. I.; Apesteguıa, C. R.; Ginés, M. J. L.; Iglesia, E. Structural Requirements and Reaction Pathways in Condensation Reactions of Alcohols on MgyAlOx Catalysts. *J. Catal.* **2000**, *190* (2), 261–275.
(16) Marcu, I. C.; Tichit, D.; Fajula, F.; Tanchoux, N. Catalytic Valorization of Bioethanol over Cu-Mg-Al Mixed Oxide Catalysts. *Catal. Today* **2009**, *147* (3–4), 231–238.
(17) León, M.; Díaz, E.; Vega, A.; Ordóñez, S.; Auroux, A. Consequences of the Iron-Aluminium Exchange on the Performance of Hydrotalcite-Derived Mixed Oxides for Ethanol Condensation. *Appl. Catal. B Environ.* **2011**, *102* (3–4), 590–599.
(18) Leon, M.; Diaz, E.; Ordonez, S. Ethanol Catalytic Condensation over Mg-Al Mixed Oxides Derived from Hydrotalcites. *Catal. Today* **2011**, *164* (1), 436–442.
(19) Marcu, I. C.; Tanchoux, N.; Fajula, F.; Tichit, D. Catalytic Conversion of Ethanol into Butanol over M-Mg-Al Mixed Oxide Catalysts (M = Pd, Ag, Mn, Fe, Cu, Sm, Yb) Obtained from LDH Precursors. *Catal. Letters* **2013**, *143* (1), 23–30.
(20) Bravo-Suárez, J. J.; Subramaniam, B.; Chaudhari, R. V. Vapor-Phase Methanol and Ethanol Coupling Reactions on CuMgAl Mixed Metal Oxides. *Appl. Catal. A Gen.* **2013**, *455*, 234–246.
(21) Riemenschneider, W.; Bolt, H. M. Organic Esters. In *Ullmann's Encyclopedia of Industrial Chemistry*; 2012; Vol. 13, pp 245–266.
(22) Macala, G. S.; Matson, T. D.; Johnson, C. L.; Lewis, R. S.; Iretskii, A. V.; Ford, P. C. Hydrogen Transfer from Supercritical Methanol over a Solid Base Catalyst: A Model for Lignin Depolymerization. *ChemSusChem* **2009**, *2* (3), 215–217.
(23) Barta, K.; Matson, T. D.; Fettig, M. L.; Scott, S. L.; Iretskii, A. V.; Ford, P. C. Catalytic Disassembly of an Organosolv Lignin via Hydrogen Transfer from Supercritical Methanol. *Green Chem.* **2010**, *12* (9), 1640.
(24) Matson, T. D.; Barta, K.; Iretskii, A. V; Ford, P. C. One-Pot Catalytic Conversion of Cellulose and of Woody Biomass Solids to Liquid Fuels. *J. Am. Chem. Soc.* **2011**, *133* (35), 14090–14097.
(25) Barta, K.; Ford, P. C. Catalytic Conversion of Nonfood Woody Biomass Solids to Organic Liquids. *Acc. Chem. Res.* **2014**, *47* (5), 1503–1512.
(26) Huang, X.; Korányi, T. I.; Boot, M. D.; Hensen, E. J. M. Catalytic Depolymerization of Lignin in Supercritical Ethanol. *ChemSusChem* **2014**, *7* (8), 2276–2288.
(27) Sun, Z.; Couto Vasconcelos, A.; Bottari, G.; Stuart, M. C. A.; Bonura, G.; Cannilla, C.; Frusteri, F.; Barta, K. Efficient Catalytic Conversion of Ethanol to 1-Butanol via the Guerbet Reaction over Copper- and Nickel-Doped Porous. *ACS Sustain. Chem. Eng.* **2016**, *5* (2), 1738–1746.
(28) Jones, Z. R.; Barrett, J. A.; Zhang, J.-P.; Ford. P.C.; Scott, S. L. Evolution of a Heterogeneous Cu-Based Lignin Hydrogenolysis Catalyst in Supercritical

Methanol. *Manuscipt. in preperation*.
(29) Barrett, J.A.; Ford, P. C.; Bernt, C. M.; Chui, M. A.; Stickelmaier, C. An Overview of Lignin Disassembly with Cu-Doped Porous Metal Oxides. Reported at the *255th National Meeting of the American Chemical Society*; March 2018; CATL 113.
(30) Barrett, J. A.; Jones, Z.; Stickelmaier, C.; Schopp, N.; Ford, P. C. Guerbet Reaction of Ethanol over Cu Doped Porous Metal Oxides: Effects of Chloride "poisoning". Reported at the *255th National Meeting of the American Chemical Society*; March 2018; CATL 341.
(31) Kozlowski, J. T.; Davis, R. J. Heterogeneous Catalysts for the Guerbet Coupling of Alcohols. *ACS Catal.* **2013**, *3* (7), 1588–1600.
(32) Veibel, S.; Nielsen, J. I. On the Mechanism of the Guerbet Reaction. *Tetrahedron* **1967**, *23* (4), 1723–1733.
(33) Bahrmann, H.; Hahn, H. D.; Mayer, D.; Frey, G. D. 2-Ethylhexanol. In *Ullmann's Encyclopedia of Industrial Chemistry*; 2013; Vol. 13, pp 1–6.
(34) Panten, J.; Surburg, H. Flavors and Fragrances, 2. Aliphatic Compounds. In *Ullmann's Encyclopedia of Industrial Chemistry*; 2015; pp 1–55.
(35) (a) Given that copper has been shown to catalyze the hydrodechlorination of chlorocarbons under reducing conditions (see refs 35b and 35c) it was our hypothesis that the same reaction would occur under these reaction conditions to produce chloride ions. Since the effect of adding this chlorocarbon on the catalytic reactivity and selectivity indeed was essentially the same as that of adding an inorganic chloride salt, this hypothesis appears to be validated. (b) Huang, C. C.; Lo, S. L.; Lien, H. L. Zero-Valent Copper Nanoparticles for Effective Dechlorination of Dichloromethane Using Sodium Borohydride as a Reductant. *Chem. Eng. J.* **2012**, 203, 95–100. (c) Śrebowata, A.; Baran, R.; Casale, S.; Kamińska, I. I.; Łomot, D.; Lisovytskiy, D.; Dzwigaj, S. Catalytic Conversion of 1,2-Dichloroethane over Bimetallic Cu-Ni Loaded BEA Zeolites. *Appl. Catal. B Environ.* **2014**, 152–153 (1), 317–327
(36) Yin, W.; Venderbosch, R. H.; Bottari, G.; Krawzcyk, K. K.; Barta, K.; Heeres, H. J. Catalytic upgrading of sugar fractions from pyrolysis oils in supercritical mono-alcohols over Cu doped porous metal oxide *Appl. Catal. B Environ.* **2015**, 166-167 (1), 56-65
(37) Patterson, A. L. The Scherrer Formula for X-Ray Particle Size Determination. *Phys. Rev.* **1939**, *56* (10), 978–982.
(38) Angelescu, E.; Pavel, O. D.; Bîrjega, R.; Florea, M.; Zăvoianu, R. The Impact of The "memory Effect" on the Catalytic Activity of Mg/Al; Mg,Zn/Al; Mg/Al,Ga Hydrotalcite-like Compounds Used as Catalysts for Cycloxene Epoxidation. *Appl. Catal. A Gen.* **2008**, *341* (1–2), 50–57.
(39) **A reviewer made the interesting observation that the XRD pattern after the reaction under comparable conditions in 95% EtOH containing 140 ppm Cl^- (SI Figure S11) does not exhibit Bragg reflections consistent with greater HTC reformation as might be expected given the higher concentration of water. While we don't have a ready explanation of this difference, it seems likely that generating water as the reaction progresses would have a different impact on HTC regeneration from CuPMO than does starting with significantly higher solvent water content. For example, the approximate Cu nanoparticle domain size, as calculated using the Scherrer equation, was 8 nm larger after reaction in 95% ethanol than that after reaction in a solution initially 100% ethanol. The more extensive Cu extraction from the lattice may disrupt the longer-range order reflected by the XRD patterns.**
(40) Kloprogge, T.; Frost, R. L.; Al-, M. Infrared and Raman Study of Interlayer Anions CO_3^{2-} , NO_3^- , SO_4^{2-} and ClO_4^- in Mg/Al-Hydrotalcite. *Am. Mineral.* **2002**, *87* (3), 623–629.
(41) Frost, R. L.; Kloprogge, J. T. Infrared Emission Spectroscopic Study of Brucite. *Spectrochim. Acta - Part A Mol. Biomol. Spectrosc.* **1999**, *55* (11), 2195–2205.
(42) Hernandez-Moreno, M. J.; Ulibarri, M. A.; Rendon, J. L.; Serna, C. J. IR Characteristics of Hydrotalcite-like Compounds. *Phys. Chem. Miner.* **1985**, *12* (1), 34–38.
(43) Loring, J. S.; Thompson, C. J.; Zhang, C.; Wang, Z.; Schaef, H. T.; Rosso, K. M. In Situ Infrared Spectroscopic Study of Brucite Carbonation in Dry to Water-Saturated Supercritical Carbon Dioxide. *J. Phys. Chem. A* **2012**, *116* (19), 4768–4777.
(44) Su, C.; Suarez, D. L. In Situ Infrared Speciation of Absorbed Carbonate on Aluminum and Iron Oxides. *Clays and Clay Miner.* **1997**, *45*, 814–825.
(45) Kandare, E.; Hossenlopp, J. M. Thermal Degradation of Acetate-Intercalated Hydroxy Double and Layered Hydroxy Salts. *Inorg. Chem.* **2006**, *45* (9), 3766–3773
(46) Serjeant, E. P.; Dempsey, B. Ionisation Constants of Organic Acids in Aqueous Solution. In *IUPAC chemical data series*; Pergamon Press: Oxford; New York, 1979; p 989
(47) Argyle, M.; Bartholomew, C. Heterogeneous Catalyst Deactivation and Regeneration: A Review. *Catalysts* **2015**, *5* (1), 145–269.
(48) Twigg, M. V.; Spencer, M. S. Deactivation of Supported Copper Metal Catalysts for Hydrogenation Reactions. *Appl. Catal. A Gen.* **2001**, *212* (1–2), 161–174.
(49) Scanlon, J. T.; Willis, D. E. Calculation of Flame Ionization Detector Relative Response Factors Using the Effective Carbon Number Concept. *J. Chromatogr. Sci.* **1985**, *23* (8), 333–340.
(50) Jorgensen, A. D.; Picel, K. C.; Stamoudis, V. C. Prediction of Gas Chromatography Flame Ionization Detector Response Factors from Molecular Structures. *Anal. Chem.* **1990**, *62* (7), 683–689.
(51) Busca, G. Bases and Basic Materials in Chemical and Environmental Processes. Liquid versus Solid Basicity. *Chem. Rev.* **2010**, *110* (4), 2217–2249.

Table of contents figure.

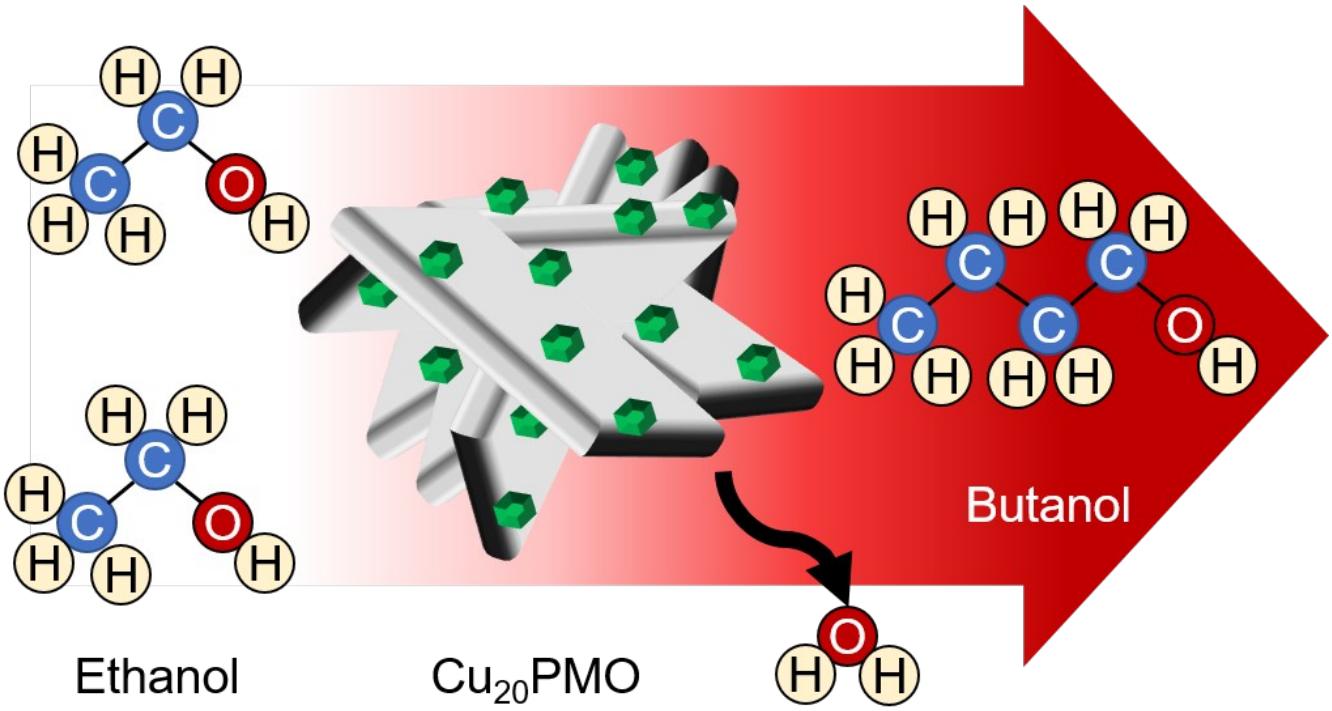

SYNOPSIS: Chloride treatment of Cu doped porous metal oxides produces a catalyst with higher activity and selectivity in the Guerbet condensation of ethanol to n-butanol. generating metal nanoparticles and decreasing overall base strength.